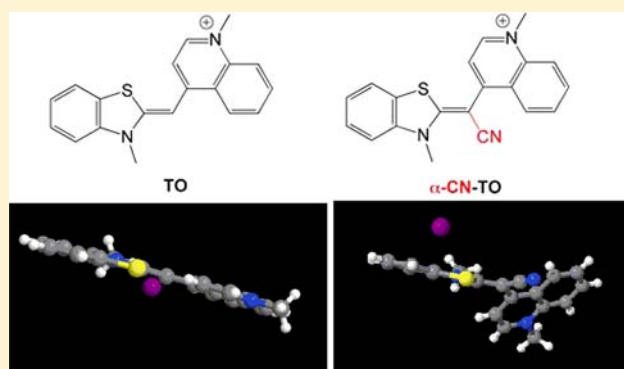# Twisted Cyanines: A Non-Planar Fluorogenic Dye with Superior Photostability and its Use in a Protein-Based Fluoromodule

Nathaniel I. Shank,[†] Ha H. Pham,[†] Alan S. Waggoner,[‡,§] and Bruce A. Armitage[†,§,*]

[†]Departments of Chemistry and [‡]Biological Sciences and [§]Molecular Biosensor and Imaging Center, Carnegie Mellon University, 4400 Fifth Avenue, Pittsburgh, Pennsylvania 15213, United States

S *Supporting Information*

ABSTRACT: The cyanine dye thiazole orange (TO) is a well-known fluorogenic stain for DNA and RNA, but this property precludes its use as an intracellular fluorescent probe for non-nucleic acid biomolecules. Further, as is the case with many cyanines, the dye suffers from low photostability. Here, we report the synthesis of a bridge-substituted version of TO named α-CN-TO, where the central methine hydrogen of TO is replaced by an electron withdrawing cyano group, which was expected to decrease the susceptibility of the dye toward singlet oxygen-mediated degradation. An X-ray crystal structure shows that α-CN-TO is twisted drastically out of plane, in contrast to TO, which crystallizes in the planar conformation. α-CN-TO retains the fluorogenic behavior of the parent dye TO in viscous glycerol/water solvent, but direct irradiation and indirect bleaching studies showed that α-CN-TO is essentially inert to visible light and singlet oxygen. In addition, the twisted conformation of α-CN-TO mitigates nonspecific binding and fluorescence activation by DNA and a previously selected TO-binding protein and exhibits low background fluorescence in HeLa cell culture. α-CN-TO was then used to select a new protein that binds and activates fluorescence from the dye. The new α-CN-TO/protein fluoromodule exhibits superior photostability to an analogous TO/protein fluoromodule. These properties indicate that α-CN-TO will be a useful fluorogenic dye in combination with specific RNA and protein binding partners for both in vitro and cell-based applications. More broadly, structural features that promote nonplanar conformations can provide an effective method for reducing nonspecific binding of cationic dyes to nucleic acids and other biomolecules.

INTRODUCTION

The number of fluorescent labels used for biological imaging has grown significantly in the past few decades, driven by the desire for multicolor labeling, increased sensitivity and functional analyses.[1−5] A number of factors are considered in developing new fluorescent labels. Ultimately, the aptitude of any label can be measured by its brightness ($\varepsilon \times \phi_F$), lack of background fluorescence/nonspecific localization, ability to withstand prolonged exposure to light and redox stresses, overall size, and ease of covalent attachment or noncovalent binding to the target of interest.

Cyanine dyes are fluorescent molecules that embody a number of desirable qualities such as high extinction coefficient, tunable absorption/emission spectra, ease of synthesis and a moderate-to-high quantum yield.[6] Over the years, these dyes have been employed as covalent and noncovalent labels. Cyanine dyes have been used as covalently attached fluorescent labels since 1989[7,8] and still see widespread use in labeling applications.[9] Noncovalent labeling methods have seen an even longer history in fluorescence spectroscopy and imaging. A well-known example of noncovalent labeling is the staining of double-stranded DNA.[10,11] The high affinity of certain cyanine

dyes toward dsDNA in solution can be attributed in part to electrostatic attraction but more significantly to the ability of the dye to intercalate between adjacent base pairs.[12,13] This interaction produces stabilizing π-stacking interactions and mitigates unfavorable hydrophobic interactions with the aqueous environment. To this end, cyanine dyes can be used as dead cell stains and in solution or in gels to detect DNA. In fact, cyanines have been reported to be able to detect DNA at picogram quantities.[10] Other researchers have developed RNA aptamers capable of binding nonintercalating fluorogenic dyes.[14−17] This could allow for the labeling of specific RNA molecules without concomitantly labeling any double stranded DNA present, as demonstrated most elegantly by the recently reported RNA aptamers that bind fluorophores based on green fluorescent protein.[18] Further, when not specifically bound by a single biomolecule, properly functionalized cyanine dyes can be noncovalently incorporated into the membranes of cells or organelles and are able to report on changes within the local environment.[19]
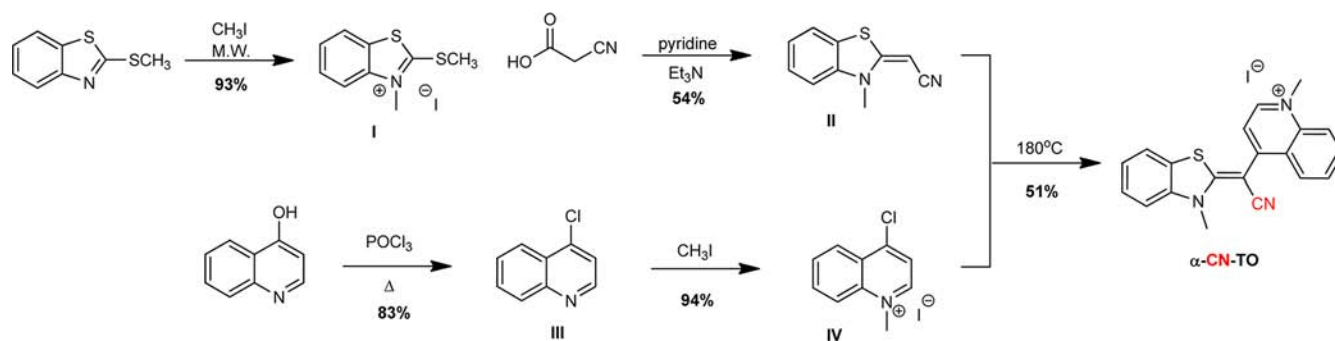
**Chart 1. Fluorogenic Cyanine Dye Structures**
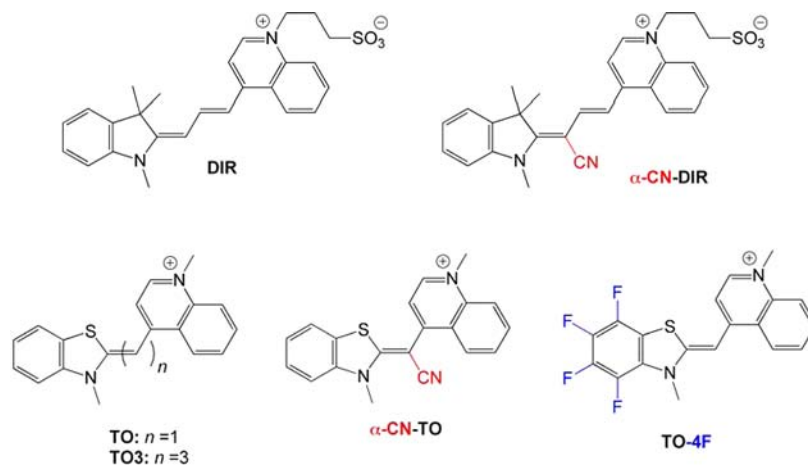
Scheme 1

Recently, dye-binding proteins have been developed to exploit the fluorogenic properties of cyanines and similar compounds in an effort to make genetically encodable fluorogenic protein tags. For example, *trans*-stilbene undergoes nonradiative excited state deactivation by isomerization, resulting in a low fluorescence quantum yield in nonviscous solution.[20,21] However, binding of *trans*-stilbene to an antibody selected against a stilbene-hapten results in up to 40-fold fluorescence enhancement.[22−24] Similarly, fluorogenic triphenylmethane and cyanine dyes have been used to select single chain variable fragment (scFv) proteins to create dye−protein pairs called fluoromodules.[25] In the original report by Szent-Gyorgyi et al., a naïve library of yeast displaying roughly 10^9 different recombinant human scFvs was challenged with either malachite green (MG) or thiazole orange (TO) to select clones capable of binding and fluorescently activating the complementary dye.[25]

The ability to rationally design fluorogenic cyanine dyes to exhibit fluorescence in virtually any desired color and the powerful selection method based on fluorescence-activated cell sorting used to identify protein partners has resulted in a diverse catalogue of fluoromodules in which the dye-protein dissociation constant (K_D) values are generally in the low-mid nanomolar range and the fluorescence quantum yields can be exceptionally high (up to $\phi_f = 1.0$).[25−28] To further increase the utility of these fluoromodules, recent efforts have focused on improving their photostability. Direct modifications to cyanine dyes with electron-withdrawing fluorine[29,30] (e.g., TO-4F in Chart 1) or cyano groups[27,31] (e.g., α-CN-DIR in Chart 1) have been used in the past to increase the stability of merocyanine

and cyanine dyes. Of the reported modifications, the attachment of an electron withdrawing cyano group in the methine bridge at the α position has proven to be particularly useful, with several-fold increases in photostability when introduced into cyanines having extended polymethine bridges.[27,31] This motivated the synthesis and characterization of a new, cyano-substituted version of thiazole orange, described herein.

■ RESULTS

Dye Synthesis. Chemical synthesis of α-CN-TO was accomplished in a total of five steps in an overall yield of 20% (Scheme 1; the alternative route, in which the central methine carbon and cyano group are provided by the quinoline heterocycle was unsuccessful). This approach requires the redesign of the synthetic route usually followed to create TO dyes, which typically involves placing the leaving group on the benzothiazole half-dye. Quaternization of the commercially available 2-methylthio-benzothiazole readily gave **I**, which reacts with cyanoacetic acid in the presence of base to undergo a malonic ester type reaction at the α carbon.[32] Spontaneous decarboxylation leads to the precipitation of the final half-dye (**II**) from aqueous solution. The commercially available 4-hydroxyquinoline was first converted to 4-chloroquinoline (**III**) in refluxing POCl_3 then quaternized with iodomethane. Electrospray ionization data showed the presence of the intended *N*-methyl-4-chloroquinolinium salt (**IV**) as well as the 4-iodo analogue, but both species should readily undergo nucleophilic aromatic substitution, so the chloro-product was not purified further. The two half-dyes were then condensed at 180 °C to give α-CN-TO as a red solid.
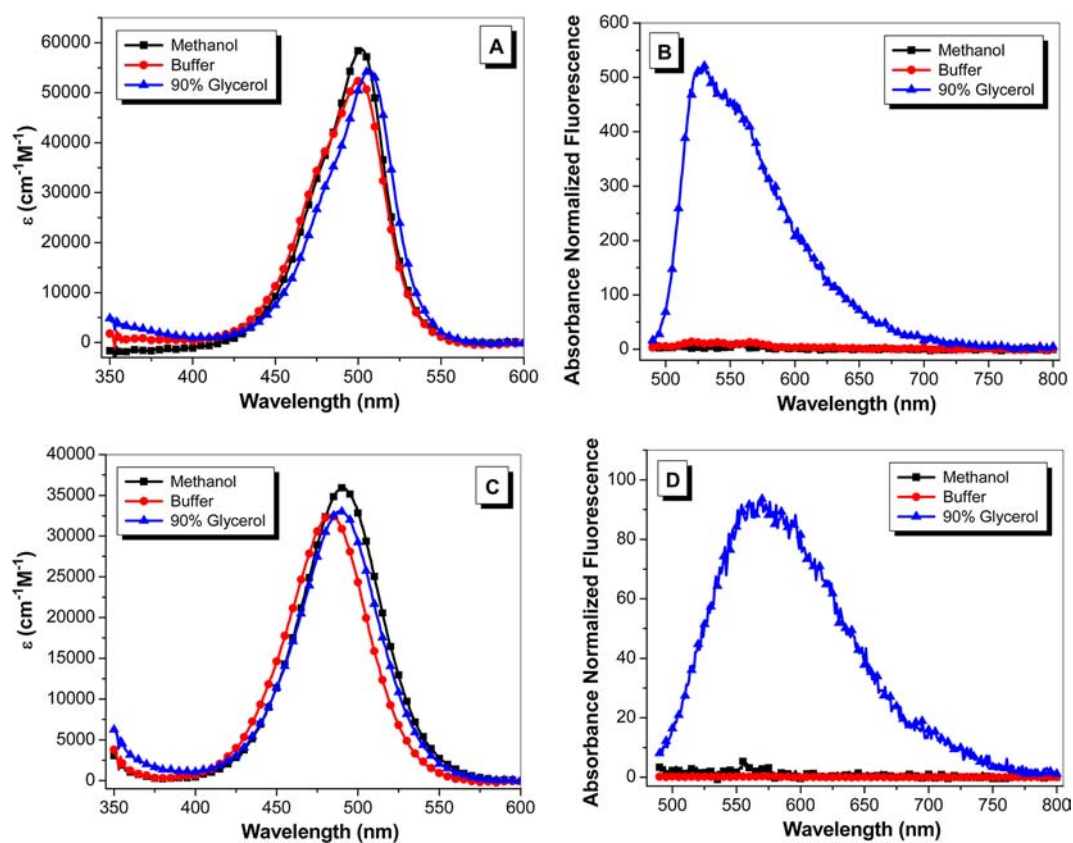
Figure 1. Absorbance and fluorescence spectra of 1 μM TO (A, B) and 2 μM α-CN-TO (C, D) in methanol, sodium phosphate buffer (pH 7.4) or 90% glycerol in water. Samples were excited at 480 nm.

Spectroscopic Characterization. We first explored the effects of the cyano substitution on the dye's absorption spectrum in homogeneous solutions (methanol, aqueous buffer, and 90% glycerol in water). It was found that the absorption band of α-CN-TO had a slight hypsochromic shift of about 16 nm compared to TO under all of the different solvent conditions (part A vs C of Figure 1). Previously reported dyes having an α-CN substitution showed much larger shifts of 40–60 nm but those dyes had longer conjugated systems than TO.[27,31] Similar to other cyano substituted dyes, the extinction coefficient of α-CN-TO decreased relative to the parent dye, in this case by approximately half ($\varepsilon_{max} = 32,500$ M^{-1}cm^{-1} in methanol). Although the extinction coefficient is decreased by α-CN modification, the modest blue-shift improves the new dye's overlap with the commonly used 488 nm laser line. In all three solvents, the absorption spectrum of α-CN-TO does not exhibit the vibrational structure normally found as a short-wavelength shoulder for monomethine cyanine dyes such as TO.

The fluorescence properties of α-CN-TO were investigated in the same solutions. Similar to other unsymmetrical cyanines, α-CN-TO exhibited very low background fluorescence in methanol and aqueous solutions.[30,33] This property is attributed to the ability of cyanine dyes to dissipate absorbed energy by rotating about the central methine carbon(s) to adopt a twisted conformation that relaxes nonradiatively to the ground state.[30,34] However, in viscous solvents or if conformationally restrained, the dyes' ability to exploit this relaxation route to return to the ground state is impeded leading to an increase in other deactivation pathways, most notably fluorescence. Parts B and D of Figure 1 show the fluorescence

spectra of TO and α-CN-TO in methanol, aqueous buffer, and 90% glycerol-in-water, a viscous medium. Whereas α-CN-TO is not as bright as TO (ca. 4-fold less based on the absorbance-normalized, integrated spectra), this result shows that the new dye is fluorogenic. Moreover, whereas TO exhibits residual fluorescence in buffer, α-CN-TO is absolutely dark.

Photostability. To assess whether or not the cyano substitution bestows the same photostability for a mono-methine dye as previously seen with trimethine dyes, we used a series of bleaching studies to compare α-CN-TO and TO in viscous (90% glycerol) and nonviscous solutions (buffer). In the first set of experiments, we irradiated each dye with white light filtered through a 380 nm long-pass filter. After 60 min of irradiation the absorbance of TO decreases by ca. 69%, whereas the spectrum of α-CN-TO was essentially unchanged (parts A and C of Figure 2). Even after accounting for the higher molar absorptivity of TO, this is a striking difference. The same experiment was next repeated in 90% glycerol. Similar to the previous experiment in nonviscous solution, TO proved to be significantly less stable than α-CN-TO bleaching by ca. 23% after 60 min (part B of Figure 2), whereas α-CN-TO exhibited no loss of fluorescence (part D of Figure 2). The higher photostability of TO in glycerol compared with buffer is likely due at least in part to the higher fluorescence quantum yield in the more viscous solvent. Another factor that could be contributing to this result is the concentration of dissolved oxygen, a major player in the photobleaching of cyanine dyes in the form of singlet oxygen generated by the dye triplet state. The concentration of oxygen is estimated to drop by 20% for a ~14% glycerol solution[35] and as much as 75% for pure glycerol.[36] Other factors, such as singlet oxygen lifetime and
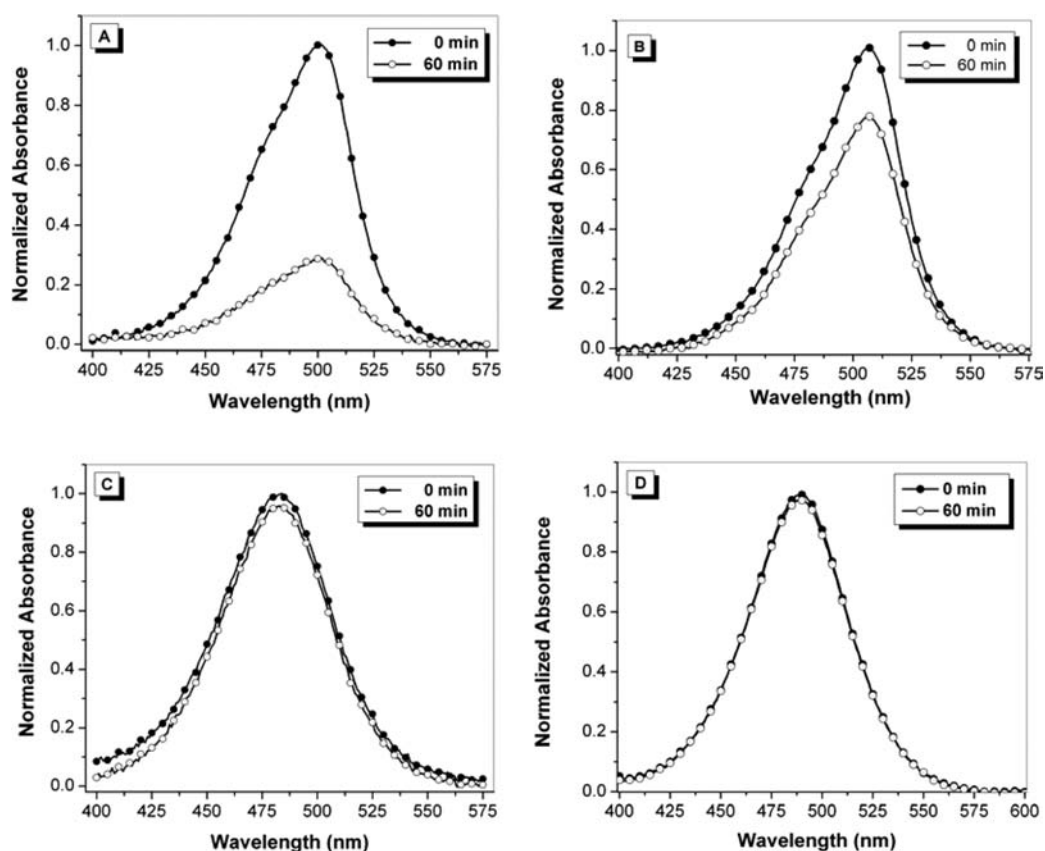
Figure 2. Photobleaching studies of TO and α-CN-TO. Absorbance spectra of 1 μM TO (A, B) and 2 μM α-CN-TO (C, D) in sodium phosphate buffer (pH 7.4) (A, C) or 90% glycerol in water (B, D) recorded before and after 60 min irradiation with visible light ($\lambda > 380$ nm).
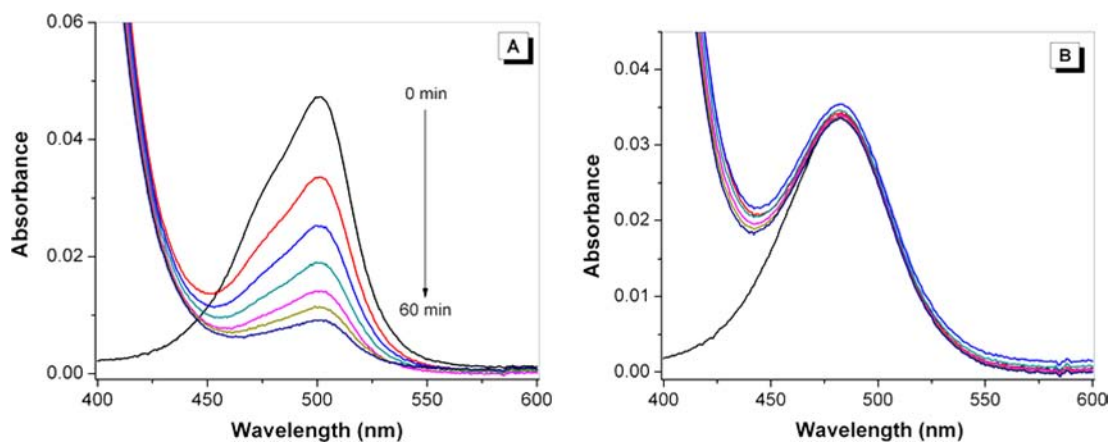
Figure 3. Time course for the bleaching of TO (A) and α-CN-TO (B) in the presence of singlet oxygen generated from molybdate and hydrogen peroxide. The rising absorption seen at short wavelengths is due to H_2O_2. Reactions were run in water with [dye] = 1 μM and pH 9; [Na_2MoO_4] = 50 mM, [H_2O_2] = 9.8 mM.

diffusion could also contribute to the difference in bleaching between these two solutions.

Singlet Oxygen Reactivity. Assuming the photobleaching of TO is due at least in part to singlet oxygen, the greater photostability of α-CN-TO could indicate lower reactivity toward singlet oxygen for the substituted dye, as we observed previously for α-CN-DIR.[27] To explore the latter pathway, we performed thermal bleaching studies on both dyes in the presence of molybdate ions, which catalytically break down hydrogen peroxide to form water and singlet oxygen via a nonphotochemical pathway.[37−39] Under these conditions TO

bleached by 82% after 60 min while α-CN-TO showed no apparent change in its UV−vis spectrum (Figure 3). Upon the basis of all of the bleaching studies, it is evident that α-CN-TO exhibits impressive photostability and is completely resistant to oxidative attack by singlet oxygen.

DNA Binding. As mentioned previously, a number of biomolecules, most notably DNA, are capable of binding and activating the fluorescence of TO. It was therefore surprising to discover that α-CN-TO gave no fluorescence in the presence of DNA while TO shows a marked increase in its signal (Figure 4). Typically, to achieve such a large apparent reduction in
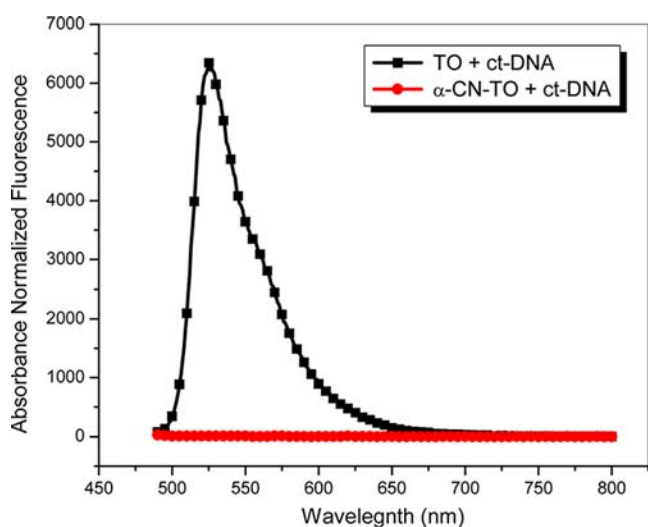
Figure 4. Fluorescence spectra of fluorogenic dyes (1 μM) in presence of calf thymus DNA (50 μM base pairs). Samples were excited at 480 nm.

affinity toward dsDNA, sterically bulky groups or negatively charged residues that provide electrostatic repulsion are installed on cyanine dyes.[17,28] Here, however, a simple bridge substitution completely eliminates the typical unsymmetrical cyanine fluorescence response. We reasoned that this lack of signal could be due to failure of α-CN-TO to intercalate into DNA as TO does or, a less likely but plausible theory, the dye is bound but in a conformation that is unfavorable for fluorescence.

We tested the possibility that α-CN-TO was binding DNA in a nonfluorescent manner by performing a competition assay. Either TO or α-CN-TO was titrated into a solution of DNA in the presence of TO-3 (Chart 1), the trimethine version of TO. TO-3 is a monocationic version of the dye TO-PRO-3 that is known to bind to DNA.[40] As shown in Figure 5, an incremental decrease in the emission of TO-3 is seen as TO is titrated into the solution. However, when α-CN-TO is titrated into the solution of DNA/TO-3, the emission spectrum of TO3 is minimally affected. These results indicate that TO can displace TO-3 from DNA but α-CN-TO cannot. Thus, it is likely that the lack of fluorescence for α-CN-TO in the presence of DNA is due to lack of binding of the dye to the DNA.

Cell Staining. To check for nonspecific staining of endogenous DNA or cellular components, we further screened both dyes against mammalian cells. Keeping the excitation intensity and detector settings fixed we imaged HeLa cells at 1 μM dye concentration without washing. Figure 6 shows that TO not only stains nuclear DNA but is also fluorescent in the mitochondria, whereas α-CN-TO shows negligible fluorescence for any cellular component. Further, the fluorescence signal for TO continues to accumulate in these areas with time (Figure S1 of the Supporting Information), whereas the images with α-CN-TO remain dark. Although it is possible that the lack of cellular fluorescence α-CN-TO is due to poor uptake of this dye by HeLa cells, this seems unlikely given the fact that both TO and α-CN-TO are monocations and have similar molecular weights. It is also noteworthy that α-CN-TO does not exhibit any obvious cytotoxic effects at low micromolar concentration.

X-ray Crystallography. The large discrepancy in apparent binding affinities for TO and α-CN-TO toward DNA led us to hypothesize that the cyano group was causing the heterocycles to be twisted out of plane at the central methine carbon because a nonplanar dye conformation would hinder intercalation between the DNA base pairs. Typically, monomethine cyanine dye conformations can be determined in solution using 2D NMR techniques, particularly observation of a nuclear Overhauser effect between the central methine proton and the quinoline ring system. However, the lack of a proton on the methine carbon in α-CN-TO precludes this approach. Fortunately, we were able to obtain crystal structures of both α-CN-TO and TO at a resolution of 0.83 Å (Figure 7). As expected, the heterocycles of TO are nearly planar and the dye adopts a conformation that projects the larger part of the quinoline system away from the sulfur heteroatom of the benzothiazole system (as drawn in Chart 1). A similar structure was reported recently for a TO derivative N-functionalized with a propanoic acid substituent on the quinoline ring.[41] In stark contrast, α-CN-TO is severely twisted with a dihedral angle between the two heterocycles of about 135° (i.e., the benzene component of the quinoline system is now closer to the benzothiazole sulfur). The inability of the nonplanar α-CN-TO to bind DNA is similar to the behavior of cyanine dyes based on dimethylindole heterocycles, where the steric bulk of the geminal methyl groups prevents intercalation. In addition, the nonplanar structure of α-CN-TO can be envisioned to render the dye more conformationally flexible than the planar TO,
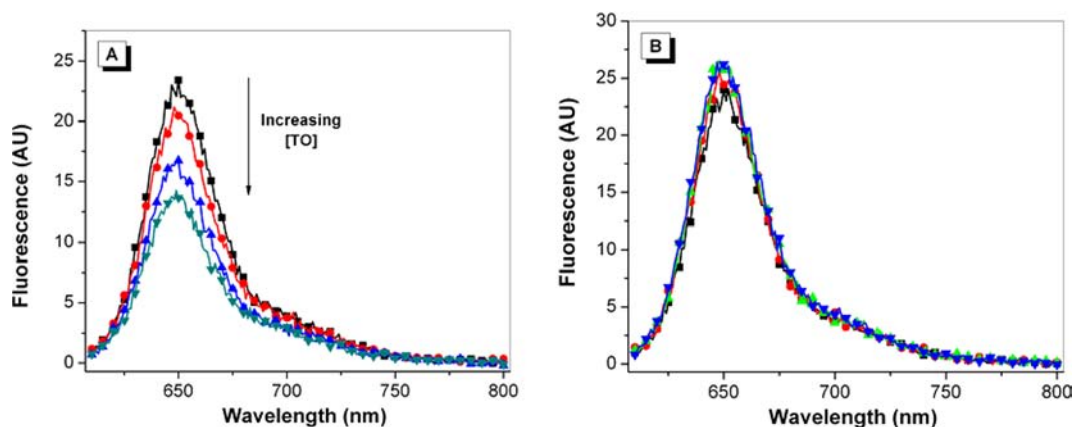
Figure 5. Competition assays between 6 μM base pairs ct-DNA and 6 μM TO-3 with TO (A) or α-CN-TO (B). Samples were excited at 590 nm.
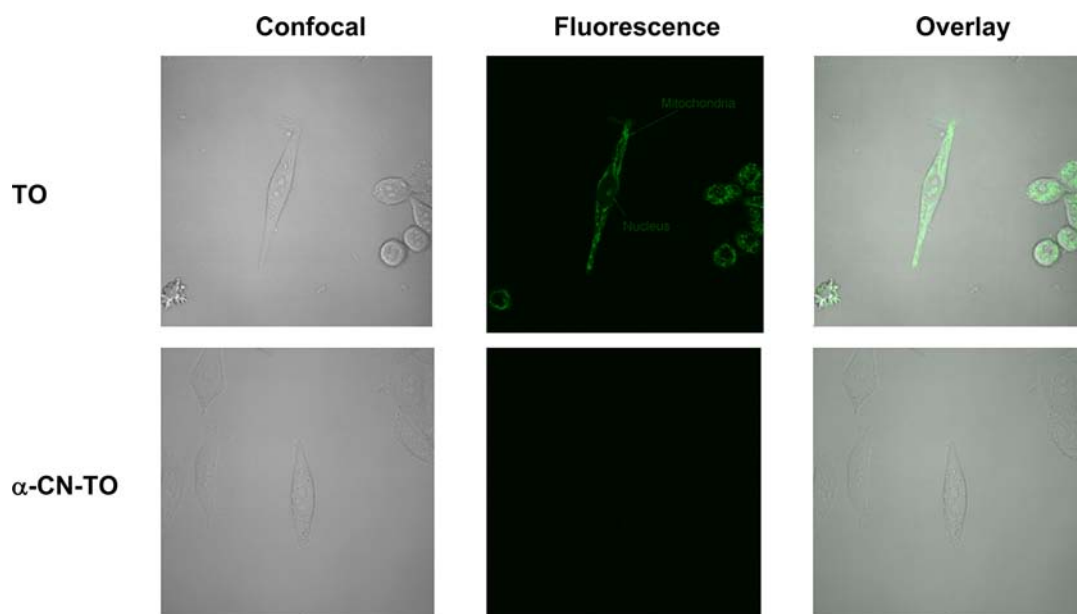
Figure 6. Confocal and fluorescence images of TO and α-CN-TO with HeLa cells. Samples were not washed before imaging. [Dye] = 1 μM.
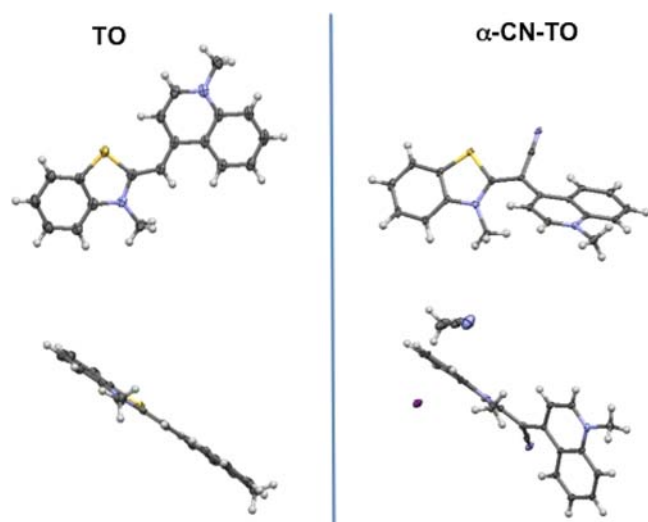
Figure 7. Crystal structures of TO (left) and α-CN-TO (right) at 0.83 Å resolution. The iodide counterion (magenta sphere) and acetonitrile solvent molecule visible in the lower right image were omitted from the upper right image for clarity. Note the proximity of the cyano group to the benzothiazole sulfur (yellow) in the upper right image.

perhaps accounting for the lack of vibrational structure in the UV−vis and fluorescence spectra shown in Figure 1.

Selection of an α-CN-TO-Binding Protein. In addition to suppressing DNA binding, the nonplanar conformation of α-CN-TO likely contributes to the failure of this dye to bind to the highly promiscuous cyanine dye-binding protein K7 (Figure S2 of the Supporting Information), which was originally isolated from a library of single-chain antibody fragments (scFv) for binding to another fluorogenic dye, dimethylindole red (DIR, Chart 1).[26] These scFv-dye complexes, known as fluoromodules, are finding increasing utility as alternatives to other protein labeling technologies. Recent applications of scFv-based fluoromodules include super-resolution imaging,[42] pH-sensitive tracking of endocytosis,[43] protease biosensing,[44]

and study of membrane receptor proteins involved in cystic fibrosis.[45−47]

Because α-CN-TO failed to bind to K7 or any other previously identified scFv we tested, we decided to use the new fluorogen as the bait to select new scFvs. As described previously, the scFv library is displayed on the surface of yeast cells and has a diversity of approximately 10^9.[25,48,49] Mixing the dye with the yeast-displayed library should result in a fluorescent halo around those yeast that display scFv proteins capable of binding and activating the dye. These winners can be separated from the rest of the library by fluorescence activated cell sorting (FACS). The individual yeast selected in this manner are allowed to reproduce, and then the enriched library is subjected to another FACS selection. The process is typically repeated 4−6 times before individual yeast are grown as isolated colonies. The gene corresponding to the selected scFv can be isolated and sequenced and then used to express and purify the scFv protein free of the yeast cell surface.
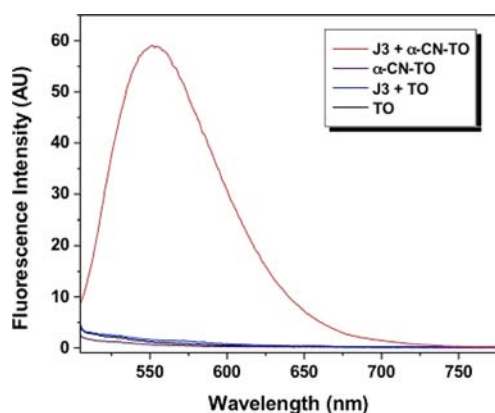
The selection process was performed to identify scFvs that activate the fluorescence of α-CN-TO. Figure 8 shows confocal fluorescence microscope images of yeast that display K7 or one of the new scFvs, J3, stained with either TO-PRO-1 or α-CN-TO. (TO-PRO-1 is a dicationic analogue of TO that was used because the monocationic TO can enter cells and fluoresce. TO-PRO-1 is known to bind to K7.[26]) A high degree of selectivity is observed: K7 only activates TO, while J3 only activates α-CN-TO. The origin of this selectivity cannot be determined without high-resolution structural analysis of the dye-protein complexes, but it is perhaps important that K7 was selected for binding to a planar fluorogen, DIR, while J3 was selected for binding to the nonplanar fluorogen α-CN-TO.

J3 was expressed and purified in soluble form. Binding of α-CN-TO to purified J3 was studied by fluorescence spectroscopy. The protein enhances the fluorescence of the dye approximately 60-fold at 100nM each of protein and dye, whereas TO exhibits almost no fluorescence (Figure 9) consistent with the cell-surface imaging experiments (Figure 8).

Finally, we compared the photostability of the α-CN-TO/J3 and TO/K7 fluoromodules. As shown in Figure 10, the α-CN-

247

dx.doi.org/10.1021/ja308629w | J. Am. Chem. Soc. 2013, 135, 242−251
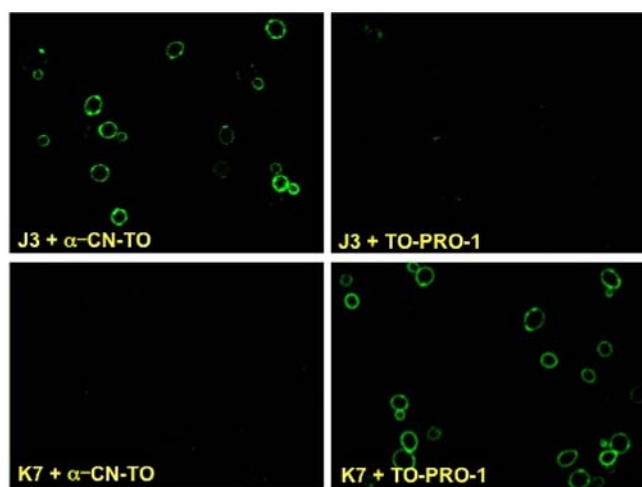
Figure 8. Confocal fluorescence microscope images of yeast displaying scFv proteins K7 or J3 at their surfaces and stained with 1 μM of either TO-PRO-1 or α-CN-TO. Images were recorded without removing excess unbound dye.

Figure 10. Photostability of α-CN-TO/J3 and TO/K7 fluoromodules. Concentrations were adjusted to give equivalent initial absorbances at the excitation wavelength of 470 $\pm$ 20 nm.
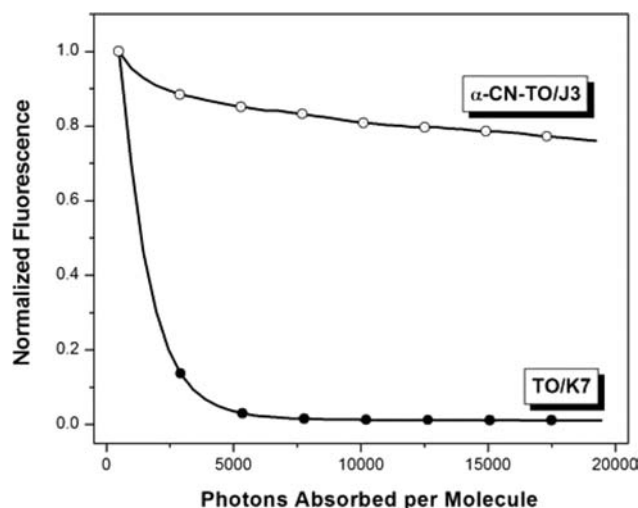

Figure 9. Fluorescence spectra of α-CN-TO and TO in the presence of purified scFv J3. [Dye] = [protein] = 500 nM. Samples were excited at 488 nm.

TO/J3 fluoromodule exhibits superior photostability by at least an order of magnitude.

■ DISCUSSION

The results presented above establish α-CN-TO as a new fluorogenic cyanine dye with high photostability. Our initial efforts to improve cyanine dye photostability relied on fluorination of the dye heterocycles, but other studies demonstrating that replacement of bridge hydrogens by electron-withdrawing cyano groups leads to larger effects motivated our synthesis of α-CN-TO. This dye shows exceptional photostability and resistance to attack by singlet oxygen, the main culprit in cyanine dye photobleaching.

The improvement in photostability upon α-cyano substitution of TO is much greater than what we observed previously for the trimethine dye DIR, where the α-cyano group enhanced photostability by a factor of 8, yet photobleaching of the dye could still be readily observed in 90% glycerol in water. The residual photobleaching of α-CN-DIR could be due to reaction of singlet oxygen at other positions on the trimethine bridge, an option that is not available in the monomethine dye α-CN-TO.

Nonplanar cyanine dyes were the subject of considerable investigation by Brooker and co-workers[50] (following earlier work by Brunings and Corwin[51]), who reported that symmetrical cyanines that are forced to adopt a nonplanar conformation exhibit red-shifted absorption spectra, while strongly unsymmetrical (i.e., cases where the basicity of the two heterocycles are significantly different) nonplanar cyanines typically exhibit blue-shifted spectra. They also predicted that nonplanar cyanines in which the heterocycles are different yet have similar basicities, as is the case for benzothiazole and quinoline,[52,53] would exhibit suppressed extinction coefficients but no significant difference in absorption maxima. α-CN-TO provides an example of such a compound, as its ε is nearly 50% lower than TO with only a minor change in λ_{max}. (The electron-withdrawing nature of the CN substituent presumably also helps to offset any red-shift that might arise from the nonplanar conformation of the dye.)

The low nonspecific binding of α-CN-TO to DNA and proteins and the absence of fluorescence when added to cell culture makes the dye an excellent candidate for selection of new scFv proteins from our yeast surface-displayed library. The preliminary characterization of one such protein, J3, supported our hypothesis that proteins could be found that would activate α-CN-TO fluorescence and exhibit improved photostability. The selection process that led to the isolation of J3 produced several other α-CN-TO-binding proteins, which we are also now characterizing.

α-CN-TO is also potentially useful for selecting genetically encodable RNA aptamers to monitor RNA expression and localization, as reported for several other fluorogens, most notably dyes modeled on the fluorescent component of GFP.[18] It should be possible to design and synthesize a family of twisted cyanines that exhibit high photostability and cover a fairly broad spectral range. We are currently in the process of synthesizing and characterizing additional α-CN-substituted monomethine cyanine dyes to broaden the catalogue of photostable, fluorogenic cyanine dyes.

■ CONCLUSIONS

In the process of improving the photostability of thiazole orange, a widely used fluorogenic cyanine dye, we discovered

that addition of an electron-withdrawing cyano group to the monomethine bridge of TO led to very high photostability, virtually no reactivity toward singlet oxygen and elimination of nonspecific DNA and protein binding leading to low background fluorescence when added to mammalian cell culture. We successfully selected a protein from a yeast-surface display library that binds and activates the fluorescence of α-CN-TO resulting in a new green fluoromodule with superior photostability to previous TO-protein complexes. Ongoing research is directed toward selecting and characterizing other α-CN-TO-binding proteins and tuning the dye structure to enhance brightness and extend the color palette of these new photostable fluoromodules.

■ EXPERIMENTAL SECTION

Reagents for the synthesis of α-CN-TO were purchased from Alfa Aesar or Sigma Aldrich and used without further purification. Solvents were HPLC grade. ^{1}H NMR spectra were recorded on a Bruker Avance 300 MHz spectrometer. High-resolution mass spectra were acquired at the CUNY Mass Spectrometry Facility at Hunter College on an Agilent Technologies G6550 iFunnel Q-TOF mass spectrometer equipped with Agilent's Jet Stream electrospray ionization source. Samples were introduced into the mass spectrometer using an Agilent Technologies 1290 UHPLC system bypassing the HPLC column. After dissolving in methanol, and diluting to an appropriate concentration, the samples were injected at 200 ul/min using 90% methanol and 10% water containing 0.1% formic acid. Settings for the ionization source were as follows; drying gas temperature 225 °C, drying gas flow 17 l/min, nebulizer pressure 20 psi, sheath gas temperature 200 °C, sheath gas flow 12 l/min, Vcap 3500 V, nozzle voltage 500 V, fragmentor 365 V. Profile and centroid mass spectral data were collected over a range of 100−1700 m/z at 2 spectra per second. The centroid data was used for the data analysis. The instrument was operated in 2 GHz wide dynamic range mode. The reference masses used were purine with M+H^{+} at 121.050873 m/z and HP 922 with M+H^{+} at 922.009798 m/z. They were infused into the spray chamber using Agilent's calibrant delivery system. The instrument was controlled with *Agilent MassHunter Workstation Acquisition Software* version B.05.00 and data was analyzed using *Agilent MassHunter Workstation Qualitative Analysis Software* version B.05.00. UV−vis and fluorescence spectra were recorded on Cary 3 and Cary Eclipse spectrophotometers respectively.

**Synthesis of α-CN-TO.** *(a). 3-Methyl-2-(methylthio)-benzothiazolium Iodide (I).* In a 15 mL pressure tube was
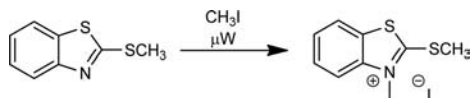
mixed 4.68 g (26 mmol) of 2-(methylthio)-benzothiazole and 10.93 g (77 mmol, 4.7 mL) of methyl iodide. The solution was reacted at 100 °C at an upper power setting of 150 W for 15 min. The heavy white precipitate was filtered and washed with ether. Yield 7.8 g (93%) ^{1}H NMR, (DMSO, δ ppm, 300 MHz): 3.13 (s, 3H), 4.11 (s, 3H), 7.72 (t, 1H, J = 7.9 Hz) 7.84 (t, 1H, J = 8.1 Hz) 8.20 (d, 1H, J = 8.5 Hz), 8.41 (d, 1H, J = 8.1 Hz).

(b). 2-(3-Methyl-2(3H)-benzothiazolylidene)-acetonitrile (II). A solution of 4.5 g (14 mmol) 3-methyl-2-(methylthio)-benzothiazolium iodide (**I**) and cyanoacetic acid were dissolved in 100 mL pyridine. After the addition of 1.41 g (14 mmol) of
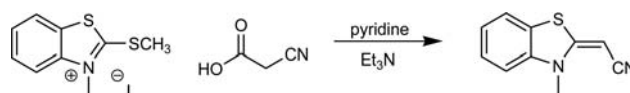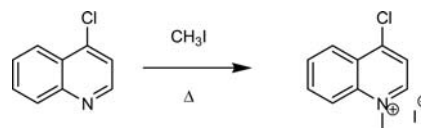

triethylamine the reaction mixture was allowed to stir overnight. Roughly 3 volumes of water were slowly added to the reaction flask with stirring during which time a homogeneous solution was obtained followed by the precipitation of the product. The solids were collected by filtration and washed thoroughly with water. Yield 1.43 g (54%) ^{1}H NMR, (CDCl₃, δ ppm, 300 MHz): 3.31 (s, 3H), 4.21 (s, 1H), 6.90 (d, 1H, J = 8.1), 7.06 (t, 1H, J = 7.5 Hz), 7.27 (t, 1H, J = 7.8 Hz), 7.38 (d, 1H, J = 7.8 Hz).

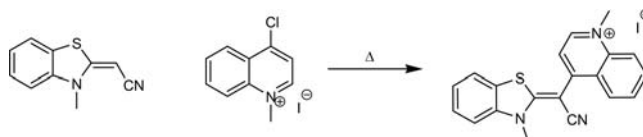*(c). 4-Chloroquinoline (III).* A neat solution of 5 g (34 mmol) of 4-hydroxyquinoline and 16 mL (~170 mmol) of
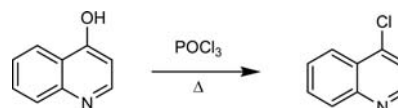
POCl₃ were heated to 110 °C for 2 h. The solution was allowed to cool to room temperature and then slowly poured onto ice. With cooling, solid sodium bicarbonate was used to neutralize the solution and precipitate the product as a fluffy white solid. The solid was filtered, washed with water, and then dried. Yield 4.67 g (83%) ^{1}H NMR, (CD₃CN, δ ppm, 300 MHz): 7.58 (d, 1H, J = 4.7 Hz), 7.70 (t, 1H, J = 7.8 Hz), 7.81 (t, 1H, J = 7.8 Hz), 8.09 (d, 1H, J = 8.4 Hz), 8.23 (d, 1H, J = 8.4), 8.77 (d, 1H, J = 4.7 Hz).

(d). N-Methyl-4-chloroquinolium Iodide (IV). In a 15 mL pressure reaction vessel was mixed 0.535 g (33 mmol) 4-

chloroquinoline (**III**) and 2.33 g (102 mmol, 1.045 mL) of methyl iodide. The tube was sealed and heated to 50 °C in an oil bath. After the appearance of a precipitate, the reaction mixture was heated for an additional hour and then allowed to cool to room temperature. Once cooled, the yellow solids were diluted further with ether and filtered. The obtained material was an inseparable mixture of 4-chloro and 4-iodo derivatives in a 1.6:1 ratio respectively. Yield (based upon 4-chloro) 0.941 g (94%) 1H NMR, (DMSO-d_6, δ ppm, 300 MHz): mixture of chloro/iodo, 4.63 (s, 3H), 8.20 (t, 1H, J = 7.6), 8.39 (t, 1H, J = 8.3), 8.52 (d, 1H, J = 6.5) 8.60 (m, 2H), 9.54 (d, 1H, 6.5).

(e). 1-Methyl-4-[(3-methyl-2(3H)-benzothiazolylidene)-cyanomethyl]-quinolinium Iodide (α-CN-TO). A homoge-

neous mixture was made from of 90 mg (0.5 mmol) 2-(3-methyl-2(3H)-benzothiazolylidene)-acetonitrile (**II**) and 152 mg (0.5 mmol) 4-chloroquinolium iodide (**IV**) in a mortar and pestle. The uniform solid was placed in a flask and heated to 150 °C for 30 min. The colored reaction was loaded directly onto a silica column and the product, an orange-red fraction, was eluted with increasing concentration of methanol (0−10%)

249

dx.doi.org/10.1021/ja308629w | J. Am. Chem. Soc. 2013, 135, 242−251

in methylene chloride. Yield 110 mg (51%) ε = 32,500 M^{-1} cm^{-1} (491 nm, methanol), ^{1}H NMR, (CD_3CN, δ ppm, 300 MHz): 3.47 (s, 3H), 4.33 (s, 3H), 7.45−7.64 (m, 4H), 7.80−7.87 (m, 2H), 8.09−8.20 (m, 2H), 8.54 (d, 1H, J = 8.5 Hz), 8.59 (d, 1H, J = 6.7 Hz). ESI-MS (M+), 330.1061 m/z, calc. 330.1065 m/z

White Light Photobleaching. Samples were irradiated with a 150 W Xe lamp using an Oriel lamp house (model #6602) equipped with a water filter (Oriel #6117) and powered by an Oriel 68805 universal power supply (40−200 W). The white light was passed through a 380 nm glass long-pass filter. Samples were immersed in an 18 ± 2 °C water bath during irradiation periods.

Thermal Bleaching. Bleaching experiments in the presence of 50 mM sodium molybdate and 9.8 mM hydrogen peroxide contained 1 mM of dye. The buffer solutions were adjusted so that the final ionic strength would be the same as the standard wash buffer with pH 9.0. Hydrogen peroxide solution (10%) was added to the buffer solution to give a final concentration of 9.8 mM. The absorbance and fluorescence spectra of the dye and protein in the buffer solution were recorded, and then Na_2MoO_4 was added to the solution. Scans were taken at 10 min intervals over a total of 60 min.

Cell Culture Imaging. HeLa cells were grown, subsequently centrifuged and resuspended in Dulbecco's modified eagle medium high glucose completed with 1% Penicillin/Streptomycin, 0.025 M HEPES Buffer Solution, and 10% Fetal Bovine Serum. 0.3 mL of the cell suspension and media were added to Lab-Tek chambered #1.0 borosilicate coverglass 8 well plates and incubated for 24 h. After the incubation the media was removed and replaced with 0.3 mL of a 1:1000 dilution of dye to media, which had been incubated until reaching 37 °C. The cells were incubated with the dye for 20 min at 37 °C, after which the well plate was imaged on the Olympus Fluoview 1000 Confocal (inverted microscope) using a 60× oil 1.42NA objective. Dyes were excited with a 488 nm laser and emissions were collected with a band-pass filter between wavelengths 505−550 nm. The photomultiplier tube levels were set to 660 V.

Selection of Yeast-Surface Display Clones That Activate α-CN-TO. The naïve yeast cell surface-display library used to select proteins that activate α-CN-TO consisted of ca. 8 × 10^{8} recombinant human scFvs made from cDNA. The library was developed by the Wittrup lab at MIT[48,49] and is also available from Pacific Northwest National Laboratory. These nonimmune scFvs were encoded in the pPNL6 plasmid as fusion protein to the yeast cell surface protein Aga2p. EBY 100 yeast strain was used to host the display library.

Expression and enrichment of αCN-TO-activating scFvs from the surface display library was performed as described previously.[25] Fluorescence Activated Cell Sorting (FACS) was conducted on a Becton Dickinson FACSVantage SE. To measure induction levels, induced cells were labeled with AlexaFluor 647 goat antimouse antibody binding to a c-myc epitope tag embedded in the scFv construct. Labeled cells were then incubated with 1 μM α-CN-TO for an hour on ice prior to sorting. A total of six rounds of enrichment and sorting were conducted. Dye concentration was reduced after each round to further enhance affinity. In the final selection round, a concentration of 100 nM α-CN-TO was used to directly sort clones onto an agar induction plate. After 3 days of growth at 20 °C, individual colonies were imaged in the presence of 1 μM

α-CN-TO. Colonies showing bright α-CN-TO fluorescence were selected for further analysis.

Fluorescence Microscopy. Frozen stock of yeast-surface displayed J3 and K7 were inoculated into 5 mL of growth medium and incubated at 30 °C. After two days, cells were induced with galactose-containing induction media for three days at 20 °C. Prior to imaging, an aliquot of 1:20 diluted induced cells was washed three times with modified PBS buffer followed by 10 min incubation with 1 μM α-CN-TO or TO-PRO-1 on ice. Yeast cells were imaged without removal of unbound dye using a Carl Zeiss LSM-510 META Confocal Microscope. Samples were excited using a 488 nm laser and a 505 nm long-pass filter. Images were processed using *ImageJ* software. False color representative of the emission window was applied.

Protein Purification. The pPNL6 plasmid containing J3 clone was extracted using Zymoprep I kit (Zymoresearch). The plasmid was then transformed into Mach1-T1[R] *E. coli*. Sequencing was performed by GeneWiz. Expression of the soluble protein was accomplished as described previously.[25]

■ ASSOCIATED CONTENT

Ⓢ Supporting Information

^{1}H NMR spectra for intermediates and α-CN-TO, time-lapse images of TO staining of HeLa cells, results of competition assays for binding of TO and α-CN-TO to the single chain antibody fragment protein K7, crystal structures of TO and α-CN-TO in thermal ellipsoid representation, fluorescence and DIC images for yeast-expressed scFv proteins stained with α-CN-TO or TO-PRO-1, and amino acid sequence of J3 protein. This material is available free of charge via the Internet at http://pubs.acs.org.

■ AUTHOR INFORMATION

Corresponding Author

*Tel: 412-268-4196, fax: 412-268-1061, e-mail: army@cmu.edu.

Notes

The authors declare no competing financial interest.

■ ACKNOWLEDGMENTS

■ REFERENCES

(1) Gonçalves, M. S. T. *Chem. Rev.* **2009**, *109*, 190−212.
(2) Suzuki, T.; Matsuzaki, T.; Hagiwara, H.; Aoki, T.; Takata, K. *Acta Histochem. Cytochem.* **2007**, *40*, 131−137.
(3) Vendrell, M.; Zhai, D.; Er, J. C.; Chang, Y.-T. *Chem. Rev.* **2012**, *112*, 4391−4420.
(4) Wysocki, L. M.; Lavis, L. D. *Curr. Opin. Chem. Biol.* **2011**, *15*, 752−759.
(5) Zhou, Y.; Xu, Z.; Yoon, J. *Chem. Soc. Rev.* **2011**, *40*, 2222−2235.
(6) Mishra, A.; Behera, R. K.; Behera, P. K.; Mishra, B. K.; Behera, G. B. *Chem. Rev.* **2000**, *100*, 1973−2011.

(7) Ernst, L. A.; Gupta, R. K.; Mujumdar, R. B.; Waggoner, A. S. *Cytometry* **1989**, *10*, 3−10.

(8) Mujumdar, R. B.; Ernst, L. A.; Mujumdar, S. T.; Waggoner, A. S. *Cytometry* **1989**, *10*, 11−19.

(9) Johnson, I.; Spence, M. T. Z. *The Molecular Probes Handbook. A Guide to Fluorescent Probes and Labeling Technologies*; 11th ed.; Invitrogen/Molecular Probes, 2010.

(10) Benson, S. C.; Mathies, R. A.; Glazer, A. N. *Nucleic Acids Res.* **1993**, *21*, 5720−5726.

(11) Rye, H. S.; Yue, S.; Wemmer, D. E.; Quesada, M. A.; Haugland, R. P.; Mathies, R. A.; Glazer, A. N. *Nucleic Acids Res.* **1992**, *20*, 2803−2812.

(12) Armitage, B. A. *Top. Heterocyc. Chem.* **2008**, *14*, 11−29.

(13) Dash, S.; Panigrahi, M.; Baliyarsingh, S.; Behera, P. K.; Patel, S.; Mishra, B. K. *Curr. Org. Chem.* **2011**, *15*, 2673−2689.

(14) Furutani, C.; Shinomiya, K.; Aoyama, Y.; Yamada, K.; Sando, S. *Mol. Biosys.* **2010**, *6*, 1569−1571.

(15) Sando, S.; Narita, A.; Aoyama, Y. *ChemBioChem* **2007**, *8*, 1795−1803.

(16) Sando, S.; Narita, A.; Hayami, M.; Aoyama, Y. *Chem. Commun.* **2008**, 3858−3860.

(17) Constantin, T.; Silva, G. L.; Robertson, K. L.; Hamilton, T. P.; Fague, K. M.; Waggoner, A. S.; Armitage, B. A. *Org. Lett.* **2008**, *10*, 1561−1564.

(18) Paige, J. S.; Wu, K. Y.; Jaffrey, S. R. *Science* **2011**, *333*, 642−646.

(19) Wilson, H. A.; Seligmann, B. E.; Chused, T. M. *J. Cell. Physiol.* **1985**, *125*, 61−71.

(20) Saltiel, J. *J. Am. Chem. Soc.* **1967**, *89*, 1036−1037.

(21) Saltiel, J.; D'Agostino, J. T. *J. Am. Chem. Soc.* **1972**, *94*, 6445−6456.

(22) Debler, E. W.; Kaufmann, G. F.; Meijler, M. M.; Heine, A.; Mee, J. M.; Pljevaljcic, G.; Di Bilio, A. J.; Schultz, P. G.; Millar, D. P.; Janda, K. D.; Wilson, I. A.; Gray, H. B.; Lerner, R. A. *Science* **2008**, *319*, 1232−1235.

(23) Simeonov, A.; Matsushita, M.; Juban, E. A.; Thompson, E. H. Z.; Hoffman, T. Z.; Beuscher, A. E., IV; Taylor, M. J.; Wirsching, P.; Rettig, W.; McCusker, J. K.; Stevens, R. C.; Millar, D. P.; Schultz, P. G.; Lerner, R. A.; Janda, K. D. *Science* **2000**, *290*, 307−313.

(24) Tian, F.; Debler, E. W.; Millar, D. P.; Deniz, A. A.; Wilson, I. A.; Schultz, P. G. *Angew. Chem., Int. Ed.* **2006**, *45*, 7763−7765.

(25) Szent-Gyorgyi, C.; Schmidt, B. F.; Creeger, Y.; Fisher, G. W.; Zakel, K. L.; Adler, S.; Fitzpatrick, J. A.; Woolford, C. A.; Yan, Q.; Vasilev, K. V.; Berget, P. B.; Bruchez, M. P.; Jarvik, J. W.; Waggoner, A. *Nat. Biotechnol.* **2007**, *26*, 235−240.

(26) Özhalici-Ünal, H.; Lee Pow, C.; Marks, S. A.; Jesper, L. D.; Silva, G. L.; Shank, N. I.; Jones, E. W.; Burnette, J. M., III; Berget, P. B.; Armitage, B. A. *J. Am. Chem. Soc.* **2008**, *130*, 12620−12621.

(27) Shank, N. I.; Zanotti, K. J.; Lanni, F.; Berget, P. B.; Waggoner, A. S.; Armitage, B. A. *J. Am. Chem. Soc.* **2009**, *131*, 12960−12969.

(28) Zanotti, K. J.; Silva, G. L.; Creeger, Y.; Robertson, K. L.; Waggoner, A. S.; Berget, P. B.; Armitage, B. A. *Org. Biomol. Chem.* **2011**, *9*, 1012−1020.

(29) Renikuntla, B. R.; Rose, H. C.; Eldo, J.; Waggoner, A. S.; Armitage, B. A. *Org. Lett.* **2004**, *6*, 909−912.

(30) Silva, G. L.; Ediz, V.; Armitage, B. A.; Yaron, D. *J. Am. Chem. Soc.* **2007**, *129*, 5710−5718.

(31) Toutchkine, A.; Nguyen, D.-V.; Hahn, K. M. *Org. Lett.* **2007**, *9*, 2775−2777.

(32) Doyle, F. P.; Kendall, J. D. Patent GB620802 (A), Great Britain, 1949.

(33) Lee, L. G.; Chen, C.; Liu, L. A. *Cytometry* **1986**, *7*, 508−517.

(34) Ediz, V.; Lee, J.; Armitage, B. A.; Yaron, D. *J. Phys. Chem. A* **2008**, *112*, 9692−9701.

(35) Kutsche, I.; Gildehaus, G.; Schuler, D.; Schumpe, A. *J. Chem. Eng. Data* **1984**, *29*, 286−287.

(36) Wilkinson, F.; Helman, W. P.; Ross, A. B. *J. Phys. Chem. Ref. Data* **1993**, *22*, 113−262.

(37) Aubry, J. M. *J. Am. Chem. Soc.* **1985**, *107*, 5844−5849.

(38) Böhme, K.; Brauer, H.-D. *Inorg. Chem.* **1992**, *31*, 3468−3471.

(39) Hayashi, Y.; Shioi, S.; Togami, M.; Sakan, T. *Chem. Lett.* **1973**, 651−654.

(40) Sovenyhazy, K. M.; Bordelon, J. A.; Petty, J. T. *Nucleic Acids Res.* **2003**, *31*, 2561−2569.

(41) Fei, X.; Gu, Y.; Lan, Y.; Shi, B.; Zhang, B. *J. Chem. Crystallogr.* **2011**, *41*, 1232−1236.

(42) Fitzpatrick, J. A. J.; Yan, Q.; Sieber, J. J.; Dyba, M.; Schwarz, U.; Szent-Gyorgyi, C.; Woolford, C. A.; Berget, P. B.; Waggoner, A. S.; Bruchez, M. P. *Bioconjugate Chem.* **2009**, *20*, 1843−1847.

(43) Grover, A.; Schmidt, B. F.; Salter, R. D.; Watkins, S. C.; Waggoner, A. S.; Bruchez, M. P. *Angew. Chem., Int. Ed.* **2012**, *51*, 4838−4842.

(44) Falco, C. N.; Dykstra, K. M.; Yates, B. P.; Berget, P. B. *Biotechnol. J.* **2009**, *4*, 1328−1336.

(45) Fisher, G. W.; Adler, S. A.; Fuhrman, M. H.; Waggoner, A. S.; Bruchez, M. P.; Jarvik, J. W. *J. Biomol. Screen.* **2010**, *15*, 703−709.

(46) Holleran, J. P.; Brown, D.; Fuhrman, M. H.; Adler, S. A.; Fisher, G. W.; Jarvik, J. W. *Cytometry Part A* **2010**, *77A*, 776−782.

(47) Holleran, J. P.; Glover, M. L.; Peters, K. W.; Bertrand, C. A.; Watkins, S. C.; Jarvik, J. W.; Frizzell, R. A. *Mol. Med.* **2012**, *18*, 685−595.

(48) Chao, G.; Lau, W. L.; Hackel, B. J.; Sazinsky, S. L.; Lippow, S. M.; Wittrup, K. D. *Nature Protocols* **2006**, *1*, 755−768.

(49) Feldhaus, M. J.; Siegel, R. W.; Opresko, L. K.; Coleman, J. R.; Feldhaus, J. M.; Yeung, Y. A.; Cochran, J. R.; Heinzelman, P.; Colby, D.; Swers, J.; Graff, C.; Wiley, H. S.; Wittrup, K. D. *Nat. Biotechnol.* **2003**, *21*, 163−170.

(50) Brooker, L. G. S.; White, F. L.; Sprague, R. H.; Dent, S. G.; Van Zandt, G. *Chem. Rev.* **1947**, *41*, 325−351.

(51) Brunings, K. J.; Corwin, A. H. *J. Am. Chem. Soc.* **1942**, *64*, 593−600.

(52) Brooker, L. G. S.; Keyes, G. H.; Williams, W. W. *J. Am. Chem. Soc.* **1942**, *64*, 199−210.

(53) Brooker, L. G. S.; Sklar, A. L.; Cressman, H. W. J.; Keyes, G. H.; Smith, L. A.; Sprague, R. H.; Van Lare, E.; Van Zandt, G.; White, F. L.; Williams, W. W. *J. Am. Chem. Soc.* **1945**, *67*, 1875−1889.